

Microstructure Evaluation and Mechanical Properties of Ti6Al4V/Inconel 718 Composites Prepared by Direct Laser Deposition

Wu Dongjiang, Yuan Shijun, Yu Chao, He Aidi, Ma Guangyi, Niu Fangyong,
Lu Fan

Key Laboratory for Precision and Non-traditional Machining Technology of Ministry of Education, Dalian University of Technology, Dalian 116024, China

Abstract: Ti6Al4V and Inconel 718 alloys are both extensively used in the aerospace industry. However, Ti6Al4V or Inconel 718 is difficult to meet the demand of both light weight and high temperature resistance. In this paper, the composites of different Ti6Al4V/Inconel 718 ratios were prepared by direct laser deposition. The phase, microstructure and element distribution were analyzed by X-ray Diffraction, scanning electron microscope and energy dispersive spectrometer, respectively. The microhardness, friction and wear properties were also investigated. With Inconel 718 content increasing, Ti₂Ni and Ni₃Ti intermetallic compound were formed. The forming mechanism of Ti₂Ni is: $\beta \rightarrow \alpha + \text{Ti}_2\text{Ni}$ and $L \rightarrow \beta\text{-Ti} + \text{Ti}_2\text{Ni}$, and the segregation mechanism of Ti₂Ni intermetallic compound is intergranular segregation. As the doping of Inconel 718 increased, the microhardness of the composites increased gradually. When the fraction of Inconel 718 is 50wt%, the average microhardness value is 7700 MPa, which is 85.5% higher than that of 100%Ti6Al4V. The increase of microhardness is directly related to Ti₂Ni intermetallic compound precipitation strengthening. Wear experiments show that the composites are dominated by abrasive wear and accompanied with adhesive wear. As Inconel 718 increased, the adhesion was weakened, and when Inconel 718 reached 50 vol%, the wear volume was just 36.9% of that of 100%Ti6Al4V.

Key words: direct laser deposition; Ti6Al4V/Inconel 718 composites; microstructure; microhardness; friction and wear

Ti6Al4V is extensively used in national defense, marine, chemical and other fields due to its high specific strength, good fatigue resistance and small coefficient of linear expansion. However, Ti6Al4V has poor high temperature performance, which severely limits its application in some high temperature environments. Inconel 718 has higher strength and oxidation resistance at high temperatures, but it has the disadvantage of lower specific strength and twice the density of Ti6Al4V. Ti6Al4V/Inconel 718 gradient materials can meet the requirements of high temperature-

lightweight and have wide application prospects. Composite materials are the basis of gradient materials, and the microstructure and mechanical properties of composite materials play an important role in the preparation of gradient materials.

At present, metal/metal and metal/ceramic functionally graded materials have been extensively studied. Ceramics are used for alloy surface modification due to their high temperature resistance, high microhardness and high temperature creep resistance. TiC_x and WC reinforcements

Received date: January 05, 2020

Foundation item: China Postdoctoral Science Foundation (2018T110215); National Key R & D Program of China (2018YFB1107801); Science Fund for Creative Research Groups of NSFC (51621064); National Natural Science Foundation of China (51805070)

Corresponding author: Ma Guangyi, Ph. D., Associate Professor, Key Laboratory for Precision and Non-traditional Machining Technology of Ministry of Education, Dalian University of Technology, Dalian 116024, P. R. China, E-mail: gyma@dlut.edu.cn

Copyright © 2021, Northwest Institute for Nonferrous Metal Research. Published by Science Press. All rights reserved.

on Ti6Al4V had been investigated by laser cladding^[1-3]. Composite coatings such as TiB+TiN/Ti and TiB₂-TiC/Ni have been prepared by the in situ reaction technology^[4,5]. Besides, ceramic such as WC, TiC reinforced Ni-based has also been investigated extensively^[6-9]. The above results indicated that ceramic coating could improve the microhardness and wear properties of the surface greatly. However, due to the large difference in thermal properties of metals and ceramics, the bonding interface is weak for its interface effect. Thus the coating spalls easily under the harsh heat cycle. Metal/metal gradient materials have broad application prospects and they have similar thermal properties. So far, nickel-based alloy/stainless steel, Ti6Al4V/Co gradient materials has been prepared by laser rapid forming^[10-13]. Ti6Al4V and stainless steel could react to form brittle phase. In order to avoid the formation of brittle phase between Ti6Al4V and stainless steel, the application of some transition layers (Ta/V/Fe, Fe/V/Cr, V/Cr/Fe) has been investigated by relevant scholars^[14-16]. The addition of some transition layers could avoid the brittle phase, which also increased the complexity of the process. Ti6Al4V-Rene88DT gradient materials were prepared by laser rapid forming and the solidification behavior and the evolution of phase were analyzed^[17]. A few studies preliminarily investigated the connection of Ti6Al4V and Inconel 718 using direct laser deposition and laser welding^[18,19]. The above studies had little discussion on its microstructure and mechanical properties. In summary, there is little research on Ti6Al4V/Inconel 718 gradient materials by direct laser deposition, especially the mechanism of formation and segregation of intermetallic compound. The mechanism of the influence of intermetallic compound on mechanical properties also needs further research.

Different ratios of Ti6Al4V and Inconel 718 composites lead to differences in microstructure and properties, and the influencing mechanisms of composites are of great significance for the formation of graded materials. In this paper, Ti6Al4V/Inconel 718 composites of different ratios were prepared by direct laser deposition. The phase, microstructure and element distribution of different compositional samples were analyzed. Further, microhardness and friction and wear properties were investigated, which laid the foundation for the preparation of functionally graded materials.

1 Experiment

The direct laser deposition system was used in the experiment, which mainly included laser device, NC machine tool and powder feeding equipment, and the working principle is shown in Fig.1. The laser device used Nd: YAG continuous laser. The powder feeder could realize to carry and blend different powders. The system used

99.99% high purity argon gas as the shielding gas and the powder carrying gas.

Ti6Al4V was used as the substrate whose size was 120 mm × 120 mm × 15 mm. Before the experiment, rough grinding was performed with SiC sandpaper, and the surface oxide layer was removed, followed by acetone washing and drying. Both Ti6Al4V and Inconel 718 powders were spherical, with the particle size range of 45~90 μm. The chemical compositions of the two powders are shown in Table 1. The powder was dried at 120 °C for 4 h before using. During the experiment, the powder feeding rate was 1.5 g/min, the scanning speed was 80~300 mm/min, the laser power was 233~420 W, the Z-axis lifting increment was 0.5~1 mm, and the sample size was 40 mm×6 mm×10 mm. Different composite materials were obtained by adjusting the process parameters.

Different volume fraction of composites (100%Ti6Al4V, 80%Ti6Al4V/20%Inconel 718, 70%Ti6Al4V/30%Inconel 718, 60%Ti6Al4V/40%Inconel 718, 50%Ti6Al4V/50%Inconel 718) were cut along the cross section and etched by Kroll reagent. The microstructure of the sample was analyzed by scanning electron microscope (SEM) and energy dispersive spectrometer (EDS). The microhardness of the composites was measured using Hv-1000 Vickers microhardness tester, of which loading force was 200 g and dwell time was 15 s. The phase composition of the sample was analyzed by XRD, and the friction and wear mechanism of components was analyzed by laser confocal microscopy.

2 Results and Discussion

2.1 Microstructure analysis

The microstructure of Ti6Al4V/Inconel 718 composites is shown in Fig.2. With the increase of Inconel 718 content, precipitates appeared in the intergranular of composites. When 718 further increased, the grains were further refined (as shown by the dashdot in Fig.2b, 2d). On the one hand, the thermal conductivity of Inconel 718 is superior to that of Ti6Al4V. With the increase of Inconel 718 content, the cooling rate was further increased, which led to grain refinement. On the other hand, due to the addition of alloying elements,

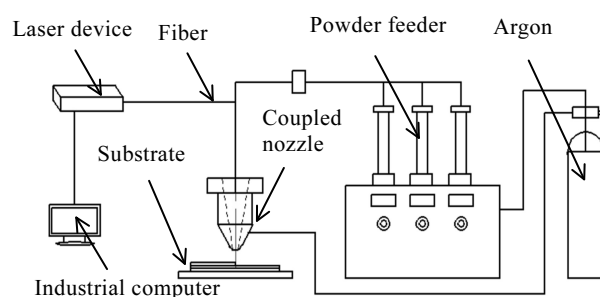


Fig.1 Principle of direct laser deposition system

Table 1 Chemical compositions of two powders (wt%)

Inconel 718	Ni	Cr	Fe	Mo	Nb
Content	50~55	17~21	Margin	2.8~3.3	4.75~5.5
Ti6Al4V	Ti	Al	V	C	Fe
Content	Bal.	5.5~6.8	3.5~4.5	0.1	0.3

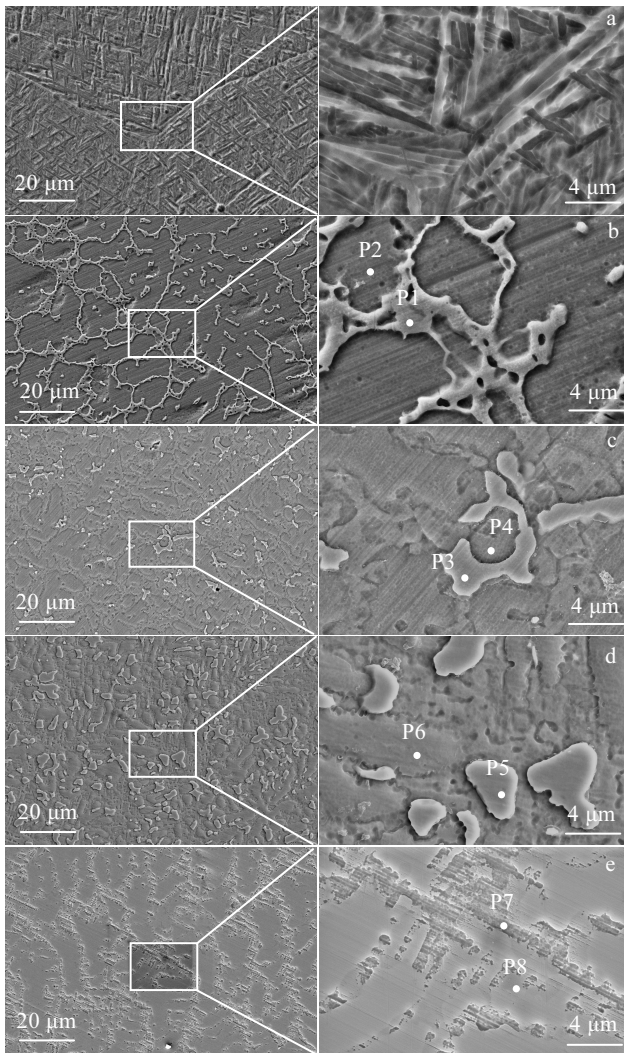


Fig.2 Microstructures of different Inconel 718 content composites: (a) 100%Ti6Al4V, (b) 20%Inconel 718/80%Ti6Al4V, (c) 30%Inconel 718/70%Ti6Al4V, (d) 40%Inconel 718/60%Ti6Al4V, and (e) 50%Inconel 718/50%Ti6Al4V

the solidification mode of the single alloy was changed, and the precipitation of intermetallic compound blocked the further growth.

Fig.2a shows the microstructure of 100%Ti6Al4V. A large amount of α -Ti lath appeared, which was due to the

high temperature gradient during direct laser deposition process, and the width of α -Ti lath reached 0.68 μm . A discrete alpha phase appeared in the beta phase between the α -Ti laths. Due to the consecutive laser deposition, solid-state annealing of the already formed metal layers may cause secondary precipitation^[17]. When the content of Inconel 718 reached 20%, as shown in Fig.2b, the microstructure was dominated by equiaxed grains. As layers increased, the cooling rate decreased^[20], accumulation of heat was increased and remelting effect was obvious, which was conducive to formation of equiaxed grains. Ti and Ni could form a dispersed second phase, which could enhance the matrix^[21]. The composition of intergranular elements and intragranular elements are shown in Table 2 (P1 and P2), and it could be seen that the intergranular Ni content was much than the intragranular.

Fig.2c is the microstructure of 30%Inconel 718/70% Ti6Al4V composite. The intergranular elements are shown in Table 2 (P3), and the atomic ratio of Ti and Ni was close to 2:1. It was judged to be Ti_2Ni intermetallic compound combined with Fig.3. The microstructure of 40%Inconel 718/60%Ti6Al4V composite is shown in Fig.2d. The intergranular elements are shown in Table 2 (P5). The atomic ratio of Ti and Ni was close to 2:1. Similarly, it was judged to be Ti_2Ni intermetallic compound combined with Fig.3. 50%Inconel718/50%Ti6Al4V microstructure is shown in Fig.2e. Element analysis indicated intergranular Ni (P7) content was much larger than the intragranular (P8).

From the above analysis, we could infer that the segregation mechanism of intermetallic compound was intergranular segregation. Ref.[22] also verified the intergranular diffusion mechanism of Ti_2Ni . Elemental analysis results did not detect Ni_3Ti intermetallic compound probably due to its little content. According to the Ni-Ti binary phase diagram (Fig.4)^[23], the formation conditions of Ni_3Ti had not been reached. Generally speaking, after the powder was melted to form molten pool, the internal elements of the

Table 2 Compositions of different points for composite material in Fig.2 (at%)

Point	Ti	Al	V	Fe	Ni	Cr
P1	63.43	5.72	1.39	4.82	23.09	1.54
P2	72.64	9.97	3.70	3.17	6.52	4.00
P3	52.46	6.12	1.83	9.63	23.93	6.04
P4	63.74	9.23	4.03	5.85	8.64	8.51
P5	50.96	6.37	1.59	11.27	22.66	7.16
P6	61.87	9.86	4.10	5.40	9.08	9.69
P7	60.10	6.42	1.12	5.64	22.76	3.97
P8	59.62	9.92	4.32	4.83	11.58	9.73

molten pool would spread evenly. The elements had not yet reached the uniform diffusion and then had begun to solidify due to the extremely high cooling rate during direct laser deposition process, which resulted in that partial region satisfied the formation conditions of Ni_3Ti intermetallic compound.

As can be seen from the titanium/nickel phase diagrams in Fig.4^[23], the addition of Ni reduced the phase transition temperature of α/β titanium from 882 °C to about 765 °C. At 765 °C, the eutectoid decomposition occurred at beginning of 5 wt% Ni: $\beta \rightarrow \alpha + Ti_2Ni$ (as shown in Fig.2b, when the volume fraction of 718 is 20vol%, the mass fraction of Ni is 18wt%). With the content of Inconel 718 increasing, eutectic reaction occurred at beginning of 28.5 wt% Ni: $L \rightarrow \beta-Ti + Ti_2Ni$ (as shown in Fig 2c~2e, when the volume fraction of 718 is 30vol%~50vol%, the mass fraction of Ni is 28wt% and 37.2wt% and 47wt%). In addition to the eutectoid reaction, the occurrence of eutectic reaction also generated Ti_2Ni .

2.2 Microhardness analysis

As shown in Fig.5, the Vickers microhardness increases linearly with increasing of Inconel 718 content. When the volume fraction of Inconel 718 reached 50vol%, the average microhardness value reached 7700 MPa and the microhardness increased by 85.5% compared to that in Ti6Al4V matrix.

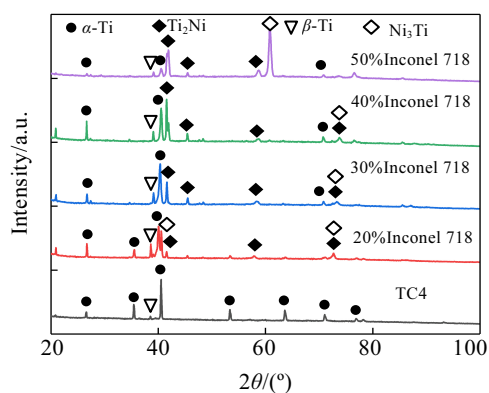


Fig.3 XRD patterns of composite materials

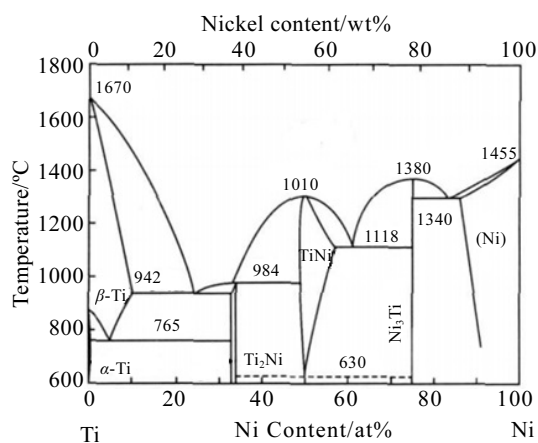


Fig.4 Titanium-nickel binary phase diagram^[23]

Ti_2Ni is a kind of harder intermetallic compound with a Vickers microhardness of about 7000 MPa, and Vickers microhardness of the forged Ti6Al4V is 3100~3300 MPa^[24,25]. The microhardness of Ti6Al4V reached 4150 MPa. In the direct laser deposition process, a large amount of $\alpha-Ti$ lath was produced. So, the microhardness value was higher than the forging.

The microhardness of the composites is directly related to the precipitation strengthening of intermetallic compound and also related to grain refinement and solid solution strengthening. The addition of alloying elements such as Ni could cause solid solution strengthening^[26]. When the volume fraction of Inconel 718 was 20vol%, the microhardness reached 5530 MPa, which was related to the formation of Ti_2Ni intermetallic compound. When the volume fraction of Inconel 718 was 30vol%, Ti_2Ni intermetallic compound content had a further increase, and the microhardness increased to 6580 MPa. As mentioned above, Ti_2Ni is a very hard intermetallic compound. In addition to precipitation strengthening of Ti_2Ni , solid solution strengthening also increased the microhardness of the composites. When the Inconel 718 content reached 40vol% and 50vol%, the microhardness reached 7100 and 7700 MPa, respectively.

2.3 Friction-wear analysis

In order to investigate the wear mechanism of the composites, the wear surfaces of composites were observed by laser confocal microscopy. The results are shown in Fig.6.

As the Inconel 718 content increased, the width of the wear surface decreased. It can be seen from Fig 6, composites had similar wear patterns, and as Inconel 718 content increased, adhesion became weaker. According to Ref. [27], the wear of Ti6Al4V mainly included adhesive wear and abrasive wear. In the actual wear process, it was often the result of a combination of various mechanisms. The wear of the surface of Ti6Al4V was in the form of peeling tearing and ploughing. According to Fig.6a, the surface of Ti6Al4V exhibited typical furrow morphology. At the beginning of wear, the hard abrasive grains were embedded in the surface of the friction pair to

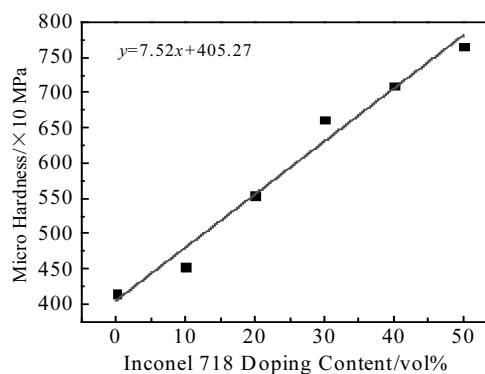


Fig.5 Vickers microhardness of the composites with different Inconel 718 volume fractions

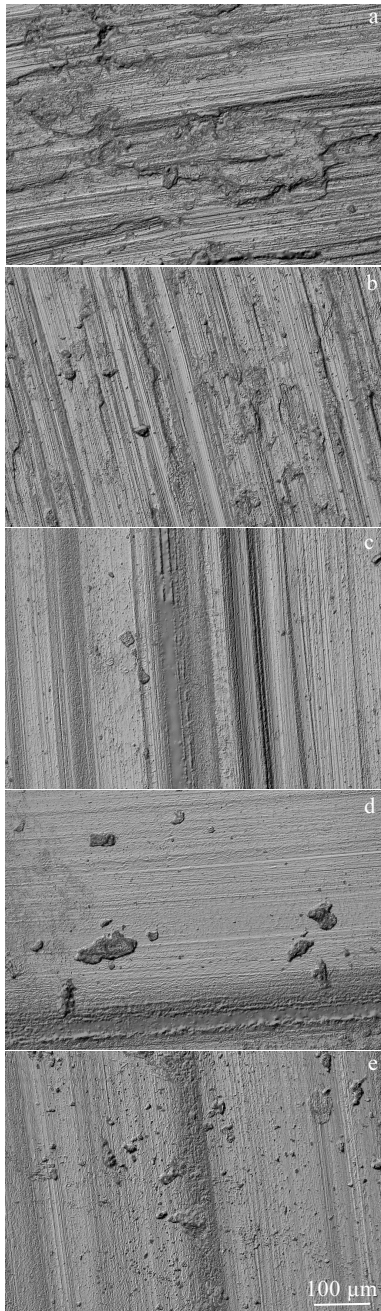


Fig 6 Wear surfaces of the composites with different Inconel 718 volume fractions: (a) 100%Ti6Al4V, (b) 20%Inconel 718/80%Ti6Al4V, (c) 30%Inconel 718/70%Ti6Al4V, (d) 40%Inconel 718/60%Ti6Al4V, and (e) 50%Inconel 718/50%Ti6Al4V

form a certain pit. Increasingly, metal adhesion occurred locally on the contact surface during sliding friction, and the adhesion was destroyed in the subsequent relative sliding, which was adhesive wear^[28]. The friction and wear mechanism was divided into three stages, and the initial wear was typical abrasive wear. As the wear time increased, the contact surface underwent plastic deformation, and the fatigue wear changed to the adhesive wear. With the Inconel

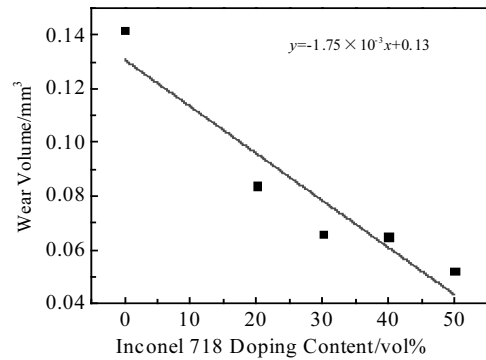


Fig.7 Wear volume of composites with different Inconel 718 volume fractions

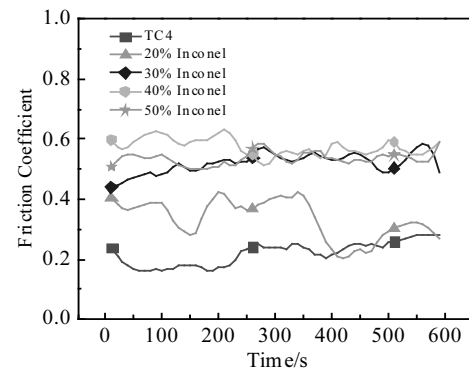


Fig.8 Friction coefficients of the composites with different Inconel 718 volume fractions

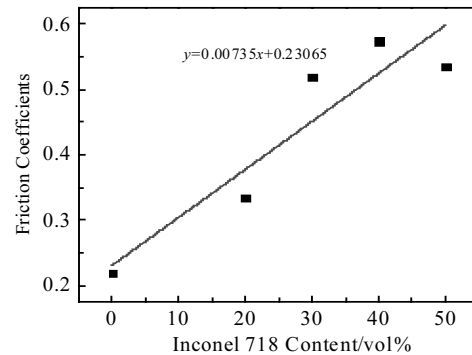


Fig.9 Changing trend of friction coefficient with Inconel 718 volume fraction

718 content increasing, the adhesive wear was weakened and the wear width was narrowed.

According to the theory of molecular mechanics, the friction coefficient included the molecular component and the mechanical component. The mechanical component has a certain relationship with the microhardness of material. Mechanical component decreases with the microhardness increasing^[29]. As the Inconel 718 content continued to increase, the microhardness of the composite increased gradually (Fig.5). The mechanical component of the

composite material was continuously reduced. The alloy with small mechanical component has less plastic deformation and weaker adhesive wear. In order to evaluate the wear resistance of composites, the calculation result of volume loss is shown in Fig.7. It can be seen that volume loss decreased linearly with the increasing Inconel 718 content. According to the above molecular theory, the content of Inconel 718 increased, the mechanical molecular component decreased, and the plastic deformation decreased, which was consistent with the tendency of the volume loss. The friction coefficients of composites with different Inconel 718 volume fractions are shown in Fig. 8. The changing trend of friction coefficient is shown in Fig. 9, and the coefficient of friction continued to rise with the content of Inconel 718 increasing. Inconel 718 has a coefficient of friction between 0.63 and 0.66^[30]. The friction coefficient increasing of composites is related to the higher friction coefficient of Inconel 718.

In summary, it can be seen that different composites had similar wear mechanisms: The wear mechanism was mainly abrasive wear. With the increase of wear time, the contact surface formed an adhesive point under the action of molecular force. Under the mechanical force, the adhesive joints were sheared, and adhesive wear occurred. According to the theory of molecular mechanics, the adhesion phenomenon decreased with the increase of Inconel 718 content. When Inconel 718 increased to 50vol%, the wear volume was 36.9% of that of 100%Ti6Al4V.

3 Conclusions

1) The composites with different ratios of Ti6Al4V/Inconel 718 composites are prepared by direct laser deposition. Precipitates appear in the intergranular of composites with the increase of Inconel 718 content.

2) With the increase of Inconel 718 content, Ti₂Ni intermetallic compound are gradually formed. The formation mechanism of Ti₂Ni is $\beta \rightarrow \alpha + \text{Ti}_2\text{Ni}$ and $L \rightarrow \beta\text{-Ti} + \text{Ti}_2\text{Ni}$, and the segregation mechanism of intermetallic compound is intergranular segregation.

3) As the content of Inconel 718 increases, the Vickers microhardness increases. When the content of Inconel 718 reaches 50vol%, the average microhardness value reaches 7700 MPa, and the microhardness increases by 85.5% compared to that of the 100%Ti6Al4V. The microhardness of the composites is directly related to the precipitation strengthening of intermetallic compound and also related to grain refinement and solid solution strengthening.

4) The wear mechanism of the composites is mainly abrasive wear, and the adhesive wear occurs as the wear time increases. With the increase of Inconel 718, the adhesion phenomenon is weakened, and when Inconel 718 increases to 50vol%, the wear volume is 36.9% of that of 100%Ti6Al4V. The coefficient of friction continues to rise with the content of Inconel 718 increasing.

References

- 1 Farayibi P K, Folkes J A, Clare A T. *Materials and Manufacturing Processes*[J], 2013, 28(5): 514
- 2 Liu S, Liu Z, Wang Y et al. *Science China Technological Sciences*[J], 2014, 57(7): 1454
- 3 Hu H D, Liu Z D, Wang L. *Materials Research Innovations*[J], 2015, 19(S9): 192
- 4 Zhao L, Cui C, Liu S et al. *Materials Science & Engineering A*[J], 2016, 663: 8
- 5 Sun R L, Niu W, Lei Y W, Tang Y. *Transactions of Materials and Heat Treatment*[J], 2012, 33(5): 131
- 6 Shu D, Li Z, Zhang K et al. *Materials Letters*[J], 2017, 195: 178
- 7 Cao S, Gu D. *Journal of Materials Research*[J], 2015, 30(23): 3616
- 8 Gu D, Cao S, Lin K. *Journal of Manufacturing Science and Engineering*[J], 2017, 139(4): 041 014
- 9 Shu D, Li Z, Yao C et al. *Surface Engineering*[J], 2018, 34(4): 276
- 10 Savitha U, Jagan Reddy G, Venkataramana A et al. *Materials Science and Engineering A*[J], 2015, 647: 344
- 11 Bonny O, Amit B. *Additive Manufacturing*[J], 2018, 22: 844
- 12 Lin X, Yue T M, Yang H O et al. *Metallurgical and Materials Transactions A*[J], 2007, 38(1): 127
- 13 Dutta Majumdar J. *Advances in Materials Science and Engineering*[J], 2011, 2011: 1
- 14 Zhang Y, Sun D Q, Gu X Y et al. *Materials Letters*[J], 2018, 212: 54
- 15 Reichardt A, Dillon R P, Borgonia J P et al. *Materials & Design*[J], 2016, 104: 404
- 16 Li W, Yan L, Karnati S et al. *Journal of Materials Processing Technology*[J], 2017, 242: 39
- 17 Lin X, Yue T M. *Materials Science and Engineering A*[J], 2005, 402(1): 294
- 18 Shah K, Haq I U, Shah S A et al. *The Scientific World Journal*[J], 2014, 201: 1
- 19 Chen H, Pinkerton A J, Li L. *The International Journal of Advanced Manufacturing Technology*[J], 2011, 52(9-12): 977
- 20 Kamara A M, Marimuthu S, Li L. *Materials and Manufacturing Processes*[J], 2014, 29(10): 1245
- 21 Wang Z X, Chen L H, Shan X L et al. *Surface Technology*[J], 2015(1): 92
- 22 Zhou Y, Yang G J, Wu X et al. *Transactions of the China Welding Institution*[J], 2010(9): 41
- 23 Okamoto H. *Phase Diagrams for Binary Alloys: A Desk Handbook*[M]. Materials Park, USA: ASM International, 2000: 314
- 24 Li A, Wang H M. *Transactions of Material and Heat Treatment*[J], 2006(5): 87
- 25 Abioye T E, Farayibi P K, Kinnel P et al. *The International Journal of Advanced Manufacturing Technology*[J], 2015, 79

- (5-8): 843
- 26 Hong X, Tan Y, Wang X et al. *Surface and Coatings Technology*[J], 2016, 305: 67
- 27 Sun Q, Hu T, Fan H et al. *Tribology International*[J], 2016, 94: 479
- 28 Xu X, Yu Y, Huang H. *Wear*[J], 2003, 255(7-12): 1421
- 29 Huang X H, Ji D J, Zhao J. *Lubrication Engineering*[J], 2011(3): 89
- 30 Zhang G, Yan S, Niu F et al. *Advanced Engineering Materials*[J], 2018, 20(4): 1 701 043

直接激光沉积 Ti6Al4V/Inconel 718 复合材料微观组织与力学性能分析

吴东江, 元世军, 余超, 何爱迪, 马广义, 牛方勇, 卢凡
(大连理工大学 精密与特种加工教育部重点实验室, 辽宁 大连 116024)

摘要: Ti6Al4V 和 Inconel 718 合金被广泛用于航空航天。但 TC4 或 Inconel 718 难以同时满足轻量化和耐高温的需求。因此采用直接激光沉积制备了不同比例 Ti6Al4V/Inconel 718 复合材料。分别通过 X 射线衍射, 扫描电子显微镜和能谱仪分析相组成, 微观结构和元素分布。同时, 研究了显微硬度和摩擦磨损性能。结果表明: 随着 Inconel 718 的比例增加, 有 Ti₂Ni 和 Ni₃Ti 金属间化合物形成。Ti₂Ni 的形成机理为: $\beta \rightarrow \alpha + \text{Ti}_2\text{Ni}$ 和 $L \rightarrow \beta\text{-Ti} + \text{Ti}_2\text{Ni}$, 且 Ti₂Ni 金属间化合物的偏析机理为晶间偏析。随着 Inconel 718 含量增加, 复合材料的显微硬度逐渐增加。当 Inconel 718 的体积分数为 50% 时, 其平均显微硬度值为 7700 MPa, 比 100%Ti6Al4V 的平均显微硬度高 85.5%。显微硬度增加与 Ti₂Ni 金属间化合物的析出强化直接相关。复合材料以磨料磨损为主, 并伴随着黏着磨损。随着 Inconel 718 的增加, 黏着磨损减弱。当 Inconel 718 的体积分数达到 50% 时, 磨损量仅为 100%Ti6Al4V 的 36.9%。

关键词: 直接激光沉积; Ti6Al4V/Inconel 718 复合材料; 微观组织; 显微硬度; 摩擦磨损

作者简介: 吴东江, 男, 1964 年生, 博士, 教授, 大连理工大学精密与特种加工教育部重点实验室, 辽宁 大连 116024, E-mail: djwudut@dlut.edu.cn